Smart Structures and Systems, *Vol. 15, No. 1 (2015) 169-189*
DOI: http://dx.doi.org/10.12989/sss.2015.15.1.169

Substructural parameters and dynamic loading identification with limited observations

Bin Xu[*1] and Jia He[1,2a]

[1]*College of Civil Engineering, Hunan University, Changsha, Hunan, China*
[2]*Department of Civil and Environmental Engineering, The Hong Kong Polytechnic University, Hong Kong, China*

(Received January 10, 2014, Revised May 9, 2014, Accepted May 25, 2014)

Abstract. Convergence difficulty and available complete measurement information have been considered as two primary challenges for the identification of large-scale engineering structures. In this paper, a time domain substructural identification approach by combining a weighted adaptive iteration (WAI) algorithm and an extended Kalman filter method with a weighted global iteration (EFK-WGI) algorithm was proposed for simultaneous identification of physical parameters of concerned substructures and unknown external excitations applied on it with limited response measurements. In the proposed approach, according to the location of the unknown dynamic loadings and the partially available structural response measurements, part of structural parameters of the concerned substructure and the unknown loadings were first identified with the WAI approach. The remaining physical parameters of the concerned substructure were then determined by EFK-WGI basing on the previously identified loadings and substructural parameters. The efficiency and accuracy of the proposed approach was demonstrated via a 20-story shear building structure and 23 degrees of freedom (DOFs) planar truss model with unknown external excitation and limited observations. Results show that the proposed approach is capable of satisfactorily identifying both the substructural parameters and unknown loading within limited iterations when both the excitation and dynamic response are partially unknown.

Keywords: substructural identification; limited observations; unknown dynamic loadings; weighted adaptive iteration algorithm; extended Kalman filter method with a weighted global iteration

1. Introduction

Detecting structural damage or fault for large scale infrastructures is an important but still challenging task because damage/fault is an intrinsically local phenomenon and the response measurement is usually limited. The research interests on the damage detection (DD), system identification (SI) and structural health monitoring (SHM) have steadily increased and extensive literature reviews can be found (Chang *et al.* 2003, Carden and Fanning 2004, Fan and Qiao 2011). In many practical situations, it is usually difficult to install sensors at all of the interested part of a structure for identification because of the complexity of the structure itself, the limitation number

∗Corresponding author, Professor, E-mail: binxu@hnu.edu.cn
[a] Postdoctoral fellow, Email: hj19830507@gmail.com

http://www.techno-press.org/?journal=sss&subpage=8 ISSN: 1738-1584 (Print), 1738-1991 (Online)

of available sensors as well as the accessibility of instrument installation. Hence, many investigators also focused on the development of SI and DD methods with incomplete measurements in time domain and/or modal domain (Yi *et al.* 2011, Lu *et al.* 2011, Park *et al.* 2011, Rahmatalla *et al.* 2012, Lei *et al.* 2012a, Xu *et al.* 2012, Yi *et al.* 2013a-b). Another widely encountered challenge for SI and DD could be ill-conditioned problem and convergence difficulty especially for large-scale structures with many unknowns involved. In practice, in many cases, only critical parts or hotspots of engineering structures, where damage is most likely to occur, need to be concerned firstly. Therefore, substructural identification (SSI) method by dividing a large structure into several smaller substructures and identifying each substructure independently has been proposed to address the aforementioned challenges (Koh *et al*. 1991, Koh *et al.* 2003, Tee *et al.* 2005, Xu 2005, Park *et al.* 2010, Law and Yong 2011).

For the purpose of possible application of the SI and DD methods in real situations, the simultaneous consideration on the aforementioned two aspects of the identification problem for large scale infrastructures would be necessary. Consequently, many researchers have contributed their efforts to develop efficient SSI approaches with incomplete measurement information. A novel substructural strategy was presented by Tee *et al.* (2009) for stiffness matrices identification and damage assessment with incomplete measurement in a divide-and-conquer manner. Lei *et al.* (2012b) proposed a damage detection method with limited input and output measurement signals and extended it for large scale structural system by employing the idea of SSI. By employing genetic algorithm (GA), Trinh and Koh (2012) presented an improved SSI strategy for large structural systems using incomplete acceleration measurements. Based on the finite element model of the intact substructure and the dynamic response reconstruction in frequency domain (Li *et al.* 2012) or wavelet domain (Li and Law 2012), two types of substructural DD approaches were proposed with incomplete measurement information. By using the Fourier transforms of two or three floor accelerations, an innovative SSI method for shear structures was proposed by Zhang and Johnson (2013), and then a modified approach, basing on the cross-power spectral densities of structural responses, was proposed by the authors (Zhang and Johnson 2012) to improve the reliability of the method when large measurement noise was involved.

In this paper, an alternative substructural identification approach by the combination of a weighted adaptive iteration (WAI) approach and an extended Kalman filter method with a weighted global iteration (EFK-WGI) was proposed for simultaneous identification of substructural physical parameters as well as the unknown external excitations applied on the concerned substructure with limited output information. In the proposed approach, according to the location of the unknown dynamic loadings and the partially available structural response measurements, part of structural parameters of the concerned substructure and the unknown loadings were first identified by using the WAI approach proposed by the authors. Subsequently, the remaining physical parameters of the concerned substructure were identified by EKF-WGI method basing on the identified loadings and substructural parameters in the previous step. The feasibility and reliability of the proposed approach was demonstrated via a 20-story shear building structure and a 23 degrees of freedom (DOFs) planar truss model with unknown external excitation and partially known response measurements. Results show that the proposed approach is capable of satisfactorily identifying both the substructural parameters and unknown loading within limited iterations when both the excitation and dynamic response are partially unknown.

2. Formulation of the proposed SSI approach with WAI and EKF-WGI

2.1 Basic idea of the SSI method

The equation of motion of a MDOFs structural system can be expressed as

$$M\ddot{x}(t)+C\dot{x}(t)+Kx(t)=f(t) \tag{1}$$

where *M*, *C*, and *K* are the mass, damping, and stiffness matrix, respectively; $\ddot{x}(t)$, $\dot{x}(t)$, and $x(t)$ are the corresponding structural acceleration, velocity, and displacement response vectors; *f*(*t*) is the external excitation vector. According to the concept of substructuring, Eq. (1) can be rearranged using partitioned matrices,

$$\begin{bmatrix} M_{ii} & M_{is} & 0 \\ M_{si} & M_{ss} & M_{sr} \\ 0 & M_{rs} & M_{rr} \end{bmatrix} \begin{Bmatrix} \ddot{x}_i(t) \\ \ddot{x}_s(t) \\ \ddot{x}_r(t) \end{Bmatrix} + \begin{bmatrix} C_{ii} & C_{is} & 0 \\ C_{si} & C_{ss} & C_{sr} \\ 0 & C_{rs} & C_{rr} \end{bmatrix} \begin{Bmatrix} \dot{x}_i(t) \\ \dot{x}_s(t) \\ \dot{x}_r(t) \end{Bmatrix} + \begin{bmatrix} K_{ii} & K_{is} & 0 \\ K_{si} & K_{ss} & K_{sr} \\ 0 & K_{rs} & K_{rr} \end{bmatrix} \begin{Bmatrix} x_i(t) \\ x_s(t) \\ x_r(t) \end{Bmatrix} = \begin{bmatrix} f_i(t) \\ f_s(t) \\ f_r(t) \end{bmatrix} \tag{2}$$

where the subscript *i* denotes interior DOFs of a concerned substructure, the subscript *s* denotes interface DOFs of the substructure with adjacent parts of the structure, and the subscript *r* denotes the remaining DOFs outside the substructure. Then, the equation of motion for the concerned substructure can be extracted from the full system as

$$\begin{bmatrix} M_{ii} & M_{is} \end{bmatrix} \begin{Bmatrix} \ddot{x}_i(t) \\ \ddot{x}_s(t) \end{Bmatrix} + \begin{bmatrix} C_{ii} & C_{is} \end{bmatrix} \begin{Bmatrix} \dot{x}_i(t) \\ \dot{x}_s(t) \end{Bmatrix} + \begin{bmatrix} K_{ii} & K_{is} \end{bmatrix} \begin{Bmatrix} x_i(t) \\ x_s(t) \end{Bmatrix} = f_i(t) \tag{3}$$

Assuming the mass distribution is known, Eq. (3) can be rewritten as

$$\begin{bmatrix} C_{ii} & C_{is} \end{bmatrix} \begin{Bmatrix} \dot{x}_i(t) \\ \dot{x}_s(t) \end{Bmatrix} + \begin{bmatrix} K_{ii} & K_{is} \end{bmatrix} \begin{Bmatrix} x_i(t) \\ x_s(t) \end{Bmatrix} = f_i(t) - \begin{bmatrix} M_{ii} & M_{is} \end{bmatrix} \begin{Bmatrix} \ddot{x}_i(t) \\ \ddot{x}_s(t) \end{Bmatrix} \tag{4}$$

This equation can be also represented as follows

$$H_{(m\times n)\times L}\theta_{L\times 1}=P_{(m\times n)\times 1} \tag{5}$$

where *H* is the response matrix composed of the velocity and displacement measurements of the concerned substructure and the interfacial DOFs; θ is the physical parameters to be identified, i.e., damping and stiffness coefficients; *m* is the number of sample points for structural dynamic response measurements; *n* is the total number of the DOFs including the DOFs in the concerned substructure and the associated interfaces; *L* is the total number of the physical parameters to be identified; and *P* is an (*m*×*n*)×1 vector composed of the external excitations and inertia forces at time *t*. Here, the force vector *P* can be expressed as

$$P=\begin{bmatrix} P(t_1) & P(t_2) & \ldots & P(t_m) \end{bmatrix}^T \tag{6}$$

in which $P(t_l) = \left[f_i(t_l) - M_{ii}\ddot{x}_i(t_l) - M_{is}\ddot{x}_s(t_l) \right]^T$ (l = 1, 2,…, m).

It is obvious from Eq. (5) that the parameters of the concerned substructure can be easily determined by any available optimization algorithms while the response measurement and the external excitation are both available. Though the input and output information of the substructure is rather reduced as compared with the whole structure, it's not always possible to obtain the complete information for SSI, e.g., only partial response of the concerned substructure is known.

The approach proposed in this paper is employed to handle the structural parameters and excitation identification problems when the dynamic response measurement of a substructure is partially unknown. Firstly, a part of a substructure with the known responses, referred to as "sub1" in the following sections, is further separated from the concerned substructure and used to simultaneously identify the unknown dynamic loading as well as the corresponding physical parameters in a priority. Subsequently, the remaining parameters of the concerned substructure are determined based on the identified parameters and the external excitation in the previous step. The details are discussed in the following sections.

2.2 WAI approach for identifying physical parameter and unknown loadings in the sub1

In practice, the force vector and the response measurement are not always completely available for identification, which means Eq. (5) cannot be directly employed for the identification. However, in some cases, it is still possible to obtain the responses of partial DOFs of the concerned substructure. Consequently, a partial substructure with known measurement information, referred to as sub1 in this study, is first separated from the concerned substructure. Similar to Eq. (5), the expression for the identification of the sub1 can be given as

$$H^{sub1}_{(m\times n)\times L}\theta^{sub1}_{L\times 1} = P^{sub1}_{(m\times n)\times L} \tag{7}$$

The force vector P^{sub1} herein is assumed to be composed of two part, i.e., the known part (P^{sub1}_{kn}) and unknown part (P^{sub1}_{un})

$$P^{sub1} = \left[P^{sub1}_{kn} \quad P^{sub1}_{un} \right]^T \tag{8}$$

where the subscript *kn* and *un* = subset consisting of the DOFs of the sub1 on which the known excitations are applied, and the DOFs on which the unknown excitations are applied, respectively. Moreover, it can be found from Eq. (7) that the estimated force vector of the sub1 on the *j*-th iteration can be determined while the estimated parameters are obtained before. Obviously, the estimated force vector on the *j*-th iteration should be composed of two corresponding parts and be shown below

$$\widetilde{P}^{sub1}_{j} = \left[\widetilde{P}^{sub1}_{kn,j} \quad \widetilde{P}^{sub1}_{un,j} \right]^T \tag{9}$$

where the symbol '~' indicates estimated values, subscript *j* means the *j*-th iteration, and subscript *kn* and *un* are defined before. Here, the above estimated force vector is firstly updated by replacing $\widetilde{P}^{sub1}_{kn,j}$ with the known part P^{sub1}_{kn} as shown in Eq. (10)

$$\hat{P}^{sub1}_{j} = \left[P^{sub1}_{kn,j} \quad \widetilde{P}^{sub1}_{un,j} \right]^T \tag{10}$$

where the symbol '^' indicates the updated values at the *j*-th iteration. In order to accelerate the convergence of the unknown excitations, the increment of the unknown external excitation identification results at the previous two iterations is employed to re-update the unknown part ($\widetilde{P}_{un,j}^{sub1}$) as shown below

$$\overline{P}_j^{sub1} = \begin{bmatrix} P_{kn,j}^{sub1} & \overline{P}_{un,j}^{sub1} \end{bmatrix}^T \tag{11}$$

in which $\overline{P}_{un,j}^{sub1} = \widetilde{P}_{un,j}^{sub1} + \beta\left(\widetilde{P}_{un,j-1}^{sub1} - \widetilde{P}_{un,j-2}^{sub1}\right)$, the symbol '-' indicates the re-updated values, and β is a learning coefficient taking the value $\beta \in [0,1)$. To avoid the ultra-iteration, the learning coefficient β employed here can be variable values. The estimated unknown excitations are getting close to the actual values when the iteration process is carried out, and then the learning coefficient should take smaller values accordingly. For simplicity, β takes the value of β / j in this paper. Since the re-updated force vector $\overline{P}_j^{sub1}$ is obtained and the response measurements are available, the physical parameters of the sub1 in the *j*-th iteration can be determined by the least-square estimation (LSE) method,

$$\widetilde{\theta}_j^{sub1} = \left[\left(H^{sub1}\right)^T H^{sub1}\right]^{-1}\left(H^{sub1}\right)^T \overline{P}_j^{sub1} \tag{12}$$

Here, to improve the convergence behavior of LSE and the accuracy of the identification results, a positive definite weight matrix defined in the following equation is introduced

$$W^{sub1} = \begin{bmatrix} aI & 0 \\ 0 & bI \end{bmatrix} \tag{13}$$

in which I = identity matrix, and a, b = weight coefficients ($a \in [1,+\infty)$, $b \in (0,1]$). The dimension of aI and bI depends on the dimension of P_{kn}^{sub1} and P_{un}^{sub1} defined before, respectively. By introducing the weight matrix to the objective function of LSE, Eq. (12) can be updated as follows

$$\widetilde{\theta}_j^{sub1} = \left[\left(H^{sub1}\right)^T W^{sub1} H^{sub1}\right]^{-1}\left(H^{sub1}\right)^T W^{sub1} \overline{P}_j^{sub1} \tag{14}$$

It can be seen that the parameters of the sub1 are identified during the iteration, and according to Eq. (7) the unknown excitations are finally determined as well in the last iteration with the identified parameters.

The basic procedure of the identification of the sub1 can be described in the following steps in which the symbol '~', '^', and '-', and superscript j are defined before.

(a) Form the response matrix H^{sub1} basing on the response measurements.

(b) Set the values of weight coefficients and learning coefficient, arbitrarily assign the initial value of the unknown excitation force for all time steps, and form the initial P vector named $\overline{P}_j^{sub1}$.

(c) According to Eq. (14) and the force vector $\overline{P}_j^{sub1}$, estimate the system parameters $\widetilde{\theta}_j^{sub1}$.

(d) Using the estimated system parameters $\widetilde{\theta}_j^{sub1}$ found in step (c), solve for the estimated force vector named $\widetilde{P}_{j+1}^{sub1}$ herein according to Eq. (7).

(e) According to Eq. (10), obtain the updated force vector $\hat{P}_{j+1}^{sub1}$ by using the partially known external excitations.

(f) If j > 2, based on $\hat{P}_{j+1}^{sub1}$, obtain $\overline{P}_{j+1}^{sub1}$ through Eq. (11); if $j \le 2$, it's unnecessary to re-updated, hence, let $\overline{P}_{j+1}^{sub1} = \hat{P}_{j+1}^{sub1}$ directly.

(g) Calculate the error between $\overline{P}_{j+1}^{sub1}$ and $\overline{P}_{j}^{sub1}$ as $e_j^{sub1} = \left\| \overline{P}_{j+1}^{sub1} - \overline{P}_{j}^{sub1} \right\|_1$ which $\|\bullet\|_1$ is the 1-norm. If the error is below an acceptable threshold, i.e. $e^j \le \varepsilon$, the procedure is complete; otherwise let $\overline{P}_{j}^{sub1} = \overline{P}_{j+1}^{sub1}$, and repeat steps (c-g).

The flowchart of the WAI approach shown in Fig. 1 helps to illustrate the procedure of the parameter and excitation identification for the sub1.

2.3 EFK-WGI algorithm for identifying the remaining parameters of the concerned substructure

Since the parameters of the sub1 and the unknown excitations applied on it are identified before, the remaining parameters of the concerned substructure can be then determined by the EKF-WGI method. For the concerned substructure, define the state vector as

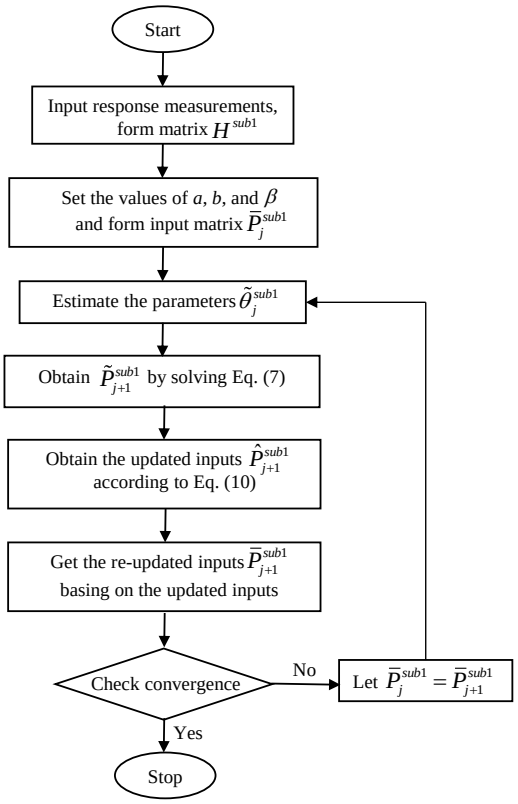

Fig. 1 Flowchart for WAI method for the parameter and loading identification of the sub1

$$\mathrm{Z}(t) = \left[x_i(t) \quad \dot{x}_i(t) \quad K' \quad C'\right]^T \tag{15}$$

where $Z(t)$ is the state vector at time t, $x_i(t)$ and $\dot{x}_i(t)$ is respectively the displacement and velocity response of the concerned substructure as mentioned in Eq. (2), K' and C' is the remaining stiffness and damping parameters, respectively, to be identified in the concerned substructure. Then, the state equation of the concerned substructure can be given as follows

$$\dot{Z}(t) = g\left[Z(t), t\right] \tag{16}$$

Suppose the observation vector at time $t_k = k \cdot \Delta t$, where Δt is the time interval, can be given as

$$y(k) = h\left(Z(t_k), t_k\right) + v(t_k) \tag{17}$$

where $y(k)$ is the observational vector at time t_k, $h\left(Z(t_k), t_k\right)$ can be considered as a function involving the state vector in accordance with the observations at time t_k, $v(t_k)$ is the observational noise vector with the covariance of ∇.

Since the state equation and the observation equation are respectively defined in Eqs. (16) and (17), a recursive process of the EKF technique can be carried out in the following steps, starting from time t_k.

(a) Start with $Z(k/k)$ and its error covariance matrix $Q(k/k)$,

(b) Evaluate the predicted state $Z(k/k+1)$ and its corresponding error covariance matrix $Q(k/k+1)$ by

$$\hat{Z}(k+1/k) = \hat{Z}(k/k) + \int_{k\cdot\Delta t}^{(k+1)\cdot\Delta t} g[\hat{Z}(k/k), t] \cdot dt \tag{18}$$

$$Q(k+1/k) = \Phi(k+1/k) \cdot Q(k/k) \cdot \Phi^T(k+1/k) \tag{19}$$

where $\Phi(k+1/k)$ is state transition matrix and can be found as follows

$$\Phi(k+1/k) \approx I + \Delta t \cdot \left[\partial g_i[Z(t), t] \Big/ \partial Z_j \right]_{Z(t)=\hat{Z}(k/k)} \tag{20}$$

(c) Estimate the Kalman gain matrix $G(k+1)$ by

$$G(k+1) = Q(k+1/k)\Psi^T(k+1/k)[\Psi(k+1/k)Q(k+1/k)\Psi^T(k+1/k) + \nabla(k+1)]^{-1} \tag{21}$$

where $\Psi(k+1/k)$ can be viewed as observation matrix and can be found as

$$\Psi(k+1/k) = \left[\partial h_i(Z(t), t) \Big/ \partial Z_j \right]_{Z(t)=\hat{Z}(k+1/k)} \tag{22}$$

(d) Estimate the filtered state $Z(k+1/k+1)$ and its error covariance matrix $Q(k+1/k+1)$ by

$$\hat{Z}(k+1/k+1) = \hat{Z}(k+1/k) + G(k+1) \cdot \left\{ y(k+1) - h\left(\hat{Z}(k+1/k), t_{k+1}\right) \right\} \tag{23}$$

$$Q(k+1/k+1)=\left[I-G(k+1)\Psi(k+1/k)\right]Q(k+1/k)\left[I-G(k+1)\Psi(k+1/k)\right]^{T}+G(k+1)\nabla(k+1)G^{T}(k+1) \tag{24}$$

(e) Take the increment $k = k+1$, and return to step (1) until $k = m$, where m represents the sample point.

Here, steps (a) to (e) mentioned before, from $k = 0$ to m, is defined as a local iteration. After this local iteration procedure is completed, a weighted global iterative procedure with an objective function is incorporated into the local EKF to obtain the stable and convergent solutions. Notably, the initial values of the state vector and the error covariance matrix in the first global iteration are the same as the local iteration, namely $Z^1(0/0)$ and $Q^1(0/0)$, where superscript 1 represents the first global iteration. However, in the second global iteration, the corresponding initial values could be

$$\hat{Z}^2(0/0)=\hat{Z}^1(m/m) \tag{25}$$

$$Q^2(0/0)=\begin{bmatrix} I & 0 \\ 0 & wQ^1_{K',C'}(m/m) \end{bmatrix} \tag{26}$$

where $\hat{Z}^1(m/m)$ is the estimation of state vector at $t_m = m\cdot\Delta t$ in the first local iteration, $Q^1_{K',C'}(m/m)$ is error covariance matrix corresponding to the parameters to be identified, w is weight used to accelerate the local iteration.

The function defined in the following equations is used to as a criterion for the termination of the global iteration.

$$\eta=\left[\sum_{i=1}^{\varsigma}(\varphi_i-\overline{\varphi})^2\right]^{1/2} \tag{27}$$

$$\overline{\varphi}=\frac{1}{\varsigma}\sum_{i=1}^{\varsigma}\varphi_i \tag{28}$$

$$\varphi_i=\frac{\sum_{k=1}^{m}\varepsilon_i^2(k)}{\sum_{k=1}^{m}y_i^2(k)} \tag{29}$$

$$\varepsilon_i(k)=y_i(k)-h\left(\hat{Z}(k/k),t_k\right) \tag{30}$$

where subscript i herein denotes the i-th observation, and ζ denotes the dimension of the observations. When the values of η is within the pre-determined threshold, the global iteration would be finished.

3. Numerical validation of the proposed SSI approach with limited observations

3.1 A 20-story shear building model

To demonstrate the efficiency and accuracy of the proposed SSI approach for simultaneous identification of the concerned substructural parameters and dynamic loadings with limited observations, a 20-story shear building model as shown in Fig. 2(a) is taken into consideration herein. The exact value of the mass distribution, inter-story stiffness, and damping coefficient corresponding to each story is set to be 100 kg, 7×10^4 N/m, and 1500 Ns/m, respectively. Without loss of the generality, a normally distributed random external excitation is assumed to be applied to the eleventh floor, and the corresponding structural response is calculated by *Newmark* method with a time interval of 0.001s.

Here, the concerned substructure is composed of the top ten floors, i.e., from the 10th floor to the 20th floor with the lower boundary of the 9th floor as shown in Fig. 2(b). The sub1 is selected to be from the 10th floor to 12th floor as shown in Fig. 2(c), and the lower boundary and upper boundary of the sub1 are respectively the 9th floor and 13th floor. The structural responses of the sub1 and the corresponding boundary are assumed to be available for the identification, and the external excitation applied on the 11th floor (i.e., f_{11} as shown in Fig. 2) is assumed to be unknown. The initial values of f_{11} are assumed to be zero which is rather different from the actual values. In the proposed SSI approach, the parameters of the sub1 and unknown loading f_{11} are firstly identified by using WAI method. The values of the weight coefficient a and b are respectively set to 10 and 0.1, and the learning coefficient β is set to 0.8. Notably, though f_{11} is assumed to be unknown, the excitations applied on the 10th floor and 12th floor are zero and then can be considered as known information for updating the estimated input vector as shown in Eqs. (9) and (10). Here, all the responses are initially assumed to be noise-free.

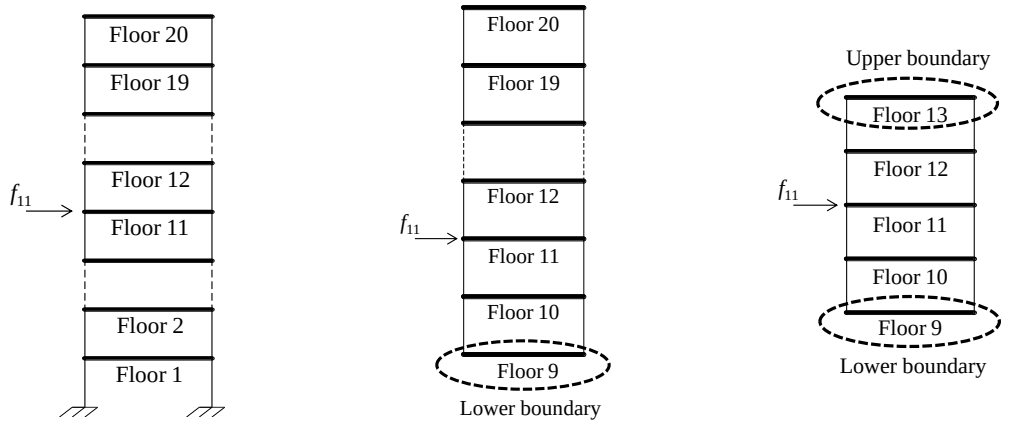

(a) The whole 20-stories structure (b) The concerned substructure (c) The sub1

Fig. 2 The 20-stories shear building structure for the numerical example

To consider the influence of the noise for the identification results, the structural response measurements in this example are also simulated by the theoretically computed responses superimposed with the corresponding white noise respectively with 3% and 5% noise-to-signal ratio in root mean square (RMS).

The structural parameters identification results of the sub1 under different noise level are shown in Table 1. It can be found from Table 1 that when the signal is noise-free, the proposed approach is capable of precisely identifying the physical parameters of the sub1. Though the identified errors are increasing as the noise level increases, the stiffness and damping coefficients can be still obtained with minor errors. The maximum identification error for stiffness is 0.29% while 3% noise is involved and 0.24% while 5% noise is involved. The maximum error for damping coefficients is a little larger, but even in the case of 5% noise level, the maximum value of errors is still only 0.66%. Fig. 3 gives the performance of the convergence during the iteration for the identification of the parameters of the sub1 when the signal is contaminated by 5% noise. Though the initial values of the unknown loadings are significantly different from the actual ones, it can be found from Fig. 3 that the estimated parameters can stably converge to their theoretical values through very limited iterations. Similar results can be obtained when the signal is noise-free and 3% noise contaminated.

Moreover, in the proposed approach, the time series of the unknown external excitation f_{11} can also be identified for the example given. The identified dynamic loading on the 11th floor of the building structure, when the response is polluted by 5% noise, is plotted in Fig. 4(a) as dashed curve, whereas the solid curve is the corresponding actual one for comparison. For clarity, only the time segment from 1s to 1.2s is plotted herein and the relative error between the identified excitation and the actual one during the whole time series is plotted in Fig. 4(b). It is obvious from Fig. 4 that the identified excitation f_{11} has a good agreement with the actual one, and similar results in the case of noise-free and 3% noise can be obtained.

Table 1 The identification results of the sub1 in the shear building structure

Parameters	Noise-free		3% noise		5% noise	
	Identified	Error (%)	Identified	Error (%)	Identified	Error (%)
k_{10}	7.00×10^4	0.00	6.99×10^4	0.14	6.98×10^4	0.29
k_{11}	7.00×10^4	0.00	6.99×10^4	0.14	6.98×10^4	0.29
k_{12}	7.00×10^4	0.00	6.98×10^4	0.29	6.97×10^4	0.43
k_{13}	7.00×10^4	0.00	6.98×10^4	0.29	6.97×10^4	0.43
c_{10}	1500.00	0.00	1497.98	0.13	1497.26	0.18
c_{11}	1500.00	0.00	1500.26	0.02	1503.68	0.25
c_{12}	1500.00	0.00	1500.63	0.04	1505.29	0.35
c_{13}	1500.00	0.00	1496.22	0.25	1490.07	0.66

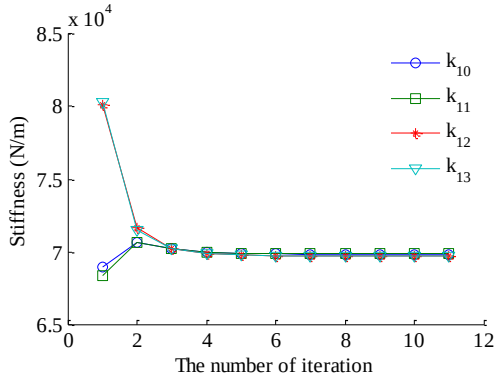

(a) The iteration for stiffness coefficients

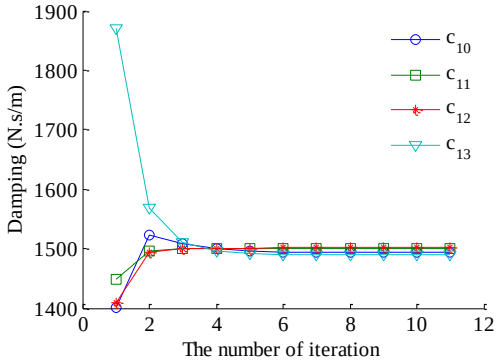

(a) The iteration for damping coefficients

Fig. 3 The convergence performance of iteration in the sub1 (5% noise)

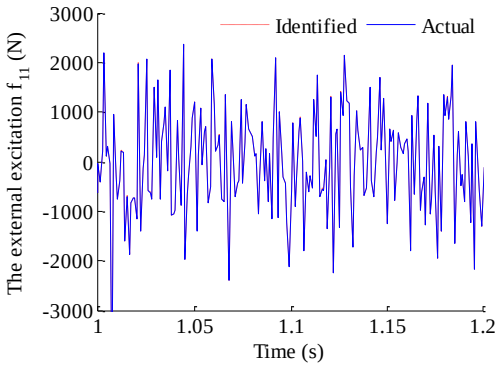

(a) Time segment of the loading

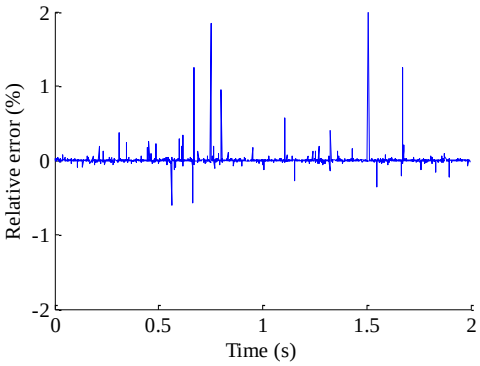

(b) The relative identified error

Fig. 4 The comparison of the identified dynamic loading in the shear building structure (5% noise)

Since the parameters of the sub1 and the unknown excitation f_{11} are identified, the remaining coefficients of the concerned substructure can be obtained by the EKF-WGI method. The state vector in this numerical example can be given as,

$$Z = \{x_{10} \quad x_{11} \quad ... \quad x_{20} \quad \dot{x}_{10} \quad \dot{x}_{11} \quad ... \quad \dot{x}_{20} \quad k_{14} \quad k_{15} \quad ... \quad k_{20} \quad c_{14} \quad c_{15} \quad ... \quad c_{20}\}^T_{36\times1} \quad (31)$$

where x_i and $\dot{x}_i$ respectively denotes the displacement and velocity of the i-th floor; k_i and c_i respectively are the stiffness and damping coefficients of the i-th floor to be identified in the concerned substructure.

As mentioned before, only the responses of the sub1 and the associated interface are assumed to be available for the identification. Consequently, in this example these measurements are considered as the observations resulting in the following observation equation,

Table 2 The identified results of the remaining parameters of the concerned substructure

Parameters	Noise-free		3% noise		5% noise	
	Identified	Error (%)	Identified	Error (%)	Identified	Error (%)
k_{14}	6.95×10^4	0.77	6.85×10^4	2.06	6.81×10^4	2.69
k_{15}	7.02×10^4	0.34	6.98×10^4	0.27	6.89×10^4	1.49
k_{16}	6.99×10^4	0.13	7.01×10^4	0.15	6.91×10^4	1.16
k_{17}	6.99×10^4	0.13	6.98×10^4	0.28	6.89×10^4	1.44
k_{18}	6.98×10^4	0.28	6.99×10^4	0.14	6.92×10^4	1.11
k_{19}	6.97×10^4	0.42	6.99×10^4	0.14	6.94×10^4	0.79
k_{20}	6.95×10^4	0.77	6.97×10^4	0.43	6.92×10^4	1.11
c_{14}	1516.65	1.11	1463.31	2.45	1399.16	6.72
c_{15}	1528.27	1.88	1558.85	3.92	1550.49	3.37
c_{16}	1524.66	1.64	1519.59	1.31	1485.78	0.95
c_{17}	1482.75	1.15	1508.81	0.59	1518.36	1.22
c_{18}	1480.15	1.32	1521.32	1.42	1548.39	3.23
c_{19}	1485.16	0.99	1517.58	1.17	1537.01	2.47
c_{20}	1481.77	1.22	1507.91	0.53	1507.91	1.28

$$y(t)=\left\{x_{10}(t) \quad ... \quad x_{13}(t) \quad \dot{x}_{10}(t) \quad ... \quad \dot{x}_{13}(t) \quad \ddot{x}_{10}(t) \quad ... \quad \ddot{x}_{13}(t)\right\}^T \tag{32}$$

The identified partial stiffness and damping coefficients of the concerned substructure (i.e., the coefficients in the sub1 identified before) provide a convenient reference for the determination of the initial value of the remaining parameters when using EKF-WGI method. Consequently, it is reasonable to assume that the initial values of the inter-story stiffness and damping are chosen to be 80% of the corresponding identified one. Moreover, to implement the EKF-WGI procedure, the error covariance matrix is $Q = 0.1\times I$, and the weight w is set to be 1000.

Similarly, three cases of noise level, saying noise-free, 3% noise and 5% noise are considered for the identification of the remaining parameters. Based on the state vector shown in Eq. (31) and the observation equation shown in Eq. (32), the remaining inter-story stiffness and damping coefficients of the concerned substructure under various noise levels are identified and shown in Table 2. It can be easily found from Table 2 that the remaining parameters of the concerned substructure can be identified with acceptable accuracy. The maximum identified errors for stiffness in the cases of the noise-free, 3% noise and 5% noise are respectively 0.77%, 2.06% and 2.69, whereas the identified errors for the damping coefficients are relatively larger with the maximum error of 1.88%, 3.92% and 6.72% in these three cases.

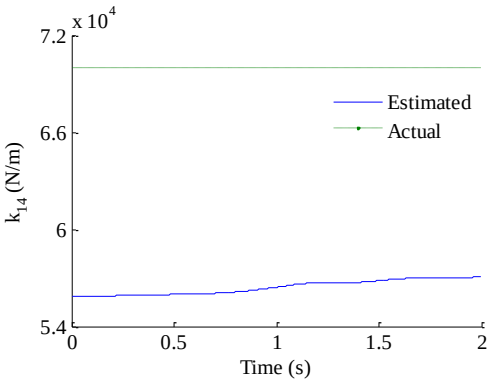

(a) The identified stiffness in the first local iteration

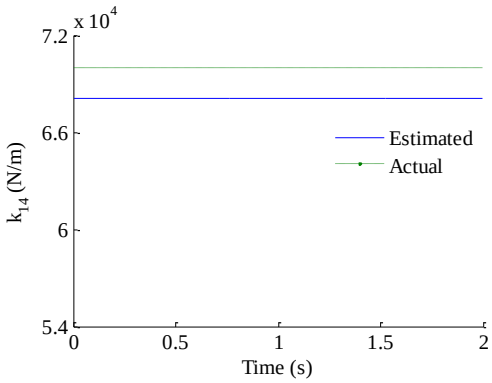

(b) The identified stiffness in the final local iteration

Fig. 5 The identified stiffness in the local iteration (5% noise)

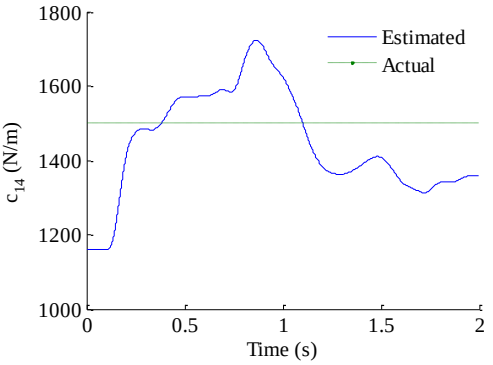

(a) The identified damping in the first local iteration

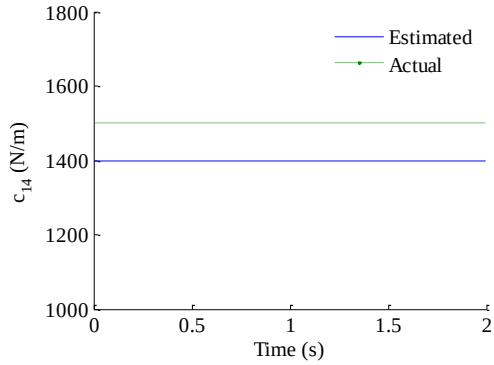

(b) The identified damping in the final local iteration

Fig. 6 The identified damping in the local iteration (5% noise)

Moreover, to investigate the changes of the identified parameters during the local iteration, Figs. 5 and 6 respectively give the performance of the first local iteration and the final local iteration on the identification of the stiffness and damping coefficients in the EKF-WGI procedure. Due to the length limitation of the paper and in order to avoid the redundant comparison, only the identified stiffness and damping coefficients of the 14th floor in the case of 5% noise are shown in Figs. 5 and 6. The dashed line represents the actual value whereas the solid line is the corresponding estimated one. For ease and clarity of the comparison of the identification results, the same scale of the coordinate is employed in both plots. It can be found from Figs. 5 and 6 that in the first local iteration the identified parameters are not correct and unstable whereas in the final local iteration the parameters are stably converged to the actual ones with acceptable accuracy. From this point of view, the EKF-WGI procedure rather than the direct employment of EKF is necessary. Furthermore, the identified results of all these remaining parameters in the global iteration are plotted in Fig. 7 to show the efficiency of the EKF-WGI method. It can be seen that though the

results in the first several global iterations are not correct, the identified parameters could be still converged to the actual one within limited global iterations.

3.2 A planar truss model with 23 members

To further investigate the reliability and applicability of the proposed approach for the simultaneous identification of the physical parameters of the concerned substructure and the dynamic loading applied on it, a planar truss model with 23 members as shown in Fig. 8(a) is introduced herein. The parameters of the truss model are given in Table 3. Similarly, a random excitation is assumed to be applied on the 8th node in the direction of DOF14 as shown in Fig. 8(a), and the corresponding structural responses are calculated by *Newmark* method with the time interval of 0.001s.

The concerned substructure in this example consists of truss members from No. 12 to No. 23 with the boundary on the 6th and 7th nodes as shown in Fig. 8(b). The sub1 is chosen to be composed of the members from No. 12 to No. 18 with the boundary on the 6th, 7th, 10th and 11th nodes as plotted in Fig. 8(c). Only the structural responses of the sub1 and the corresponding boundary are assumed to be available for the identification. The external excitation f_{14} is assumed to be unknown, and its initial values are also assumed to be zero herein. The values of the weight coefficient a and b for WAI approach are respectively set to be 10 and 0.1, and the learning coefficient β is set to 0.8. It should be noted that though f_{14} is assumed to be unknown, the excitations applied on the 8th and 9th nodes in the direction of DOF13, DOF15 and DOF16 are zero. This implicit information can be used to update the estimated input vector as shown in Eqs. (9)-(10). Here, all the responses are initially assumed to be noise-free. For practical consideration, the theoretically computed responses are also superimposed with the corresponding white noise respectively with 3% and 5% noise-to-signal ratio in RMS.

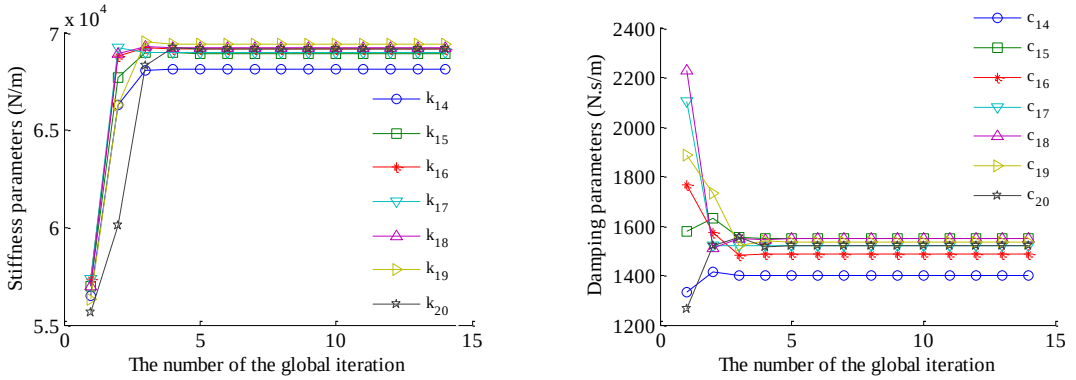

(a) The identified stiffness in the global iteration (b) The identified damping in the global iteration

Fig. 7 All the identified remaining parameters in the global iteration (5% noise)

Table 3 The parameters of the planar truss model

Element number	m (kg)	k (N/m)	c (N.s/m)	α	Element number	m (kg)	c (N/m)	c (N.s/m)	α
1	96.0	8.0×10^4	1250.0	$\pi/4$	13	115.2	9.0×10^4	1500.0	$\pi/4$
2	103.2	8.4×10^4	1300.0	0	14	98.4	9.2×10^4	1400.0	0
3	108.0	7.2×10^4	1200.0	$3\pi/4$	15	100.8	8.4×10^4	1600.0	$3\pi/4$
4	105.6	9.0×10^4	1500.0	0	16	117.6	7.6×10^4	1450.0	0
5	110.4	8.8×10^4	1400.0	$\pi/4$	17	108.0	7.6×10^4	1550.0	$\pi/4$
6	112.8	8.6×10^4	1350.0	0	18	112.8	8.6×10^4	1350.0	0
7	108.0	7.6×10^4	1550.0	$3\pi/4$	19	110.1	8.8×10^4	1400.0	$3\pi/4$
8	117.6	7.6×10^4	1450.0	0	20	105.6	9.0×10^4	1500.0	0
9	100.8	8.4×10^4	1600.0	$\pi/4$	21	108.0	7.2×10^4	1200.0	$\pi/4$
10	98.4	9.2×10^4	1400.0	0	22	103.2	8.4×10^4	1300.0	0
11	115.2	9.0×10^4	1500.0	$3\pi/4$	23	96.0	8.0×10^4	1250.0	$3\pi/4$
12	103.2	9.6×10^4	1700.0	0	--	--	--	--	--

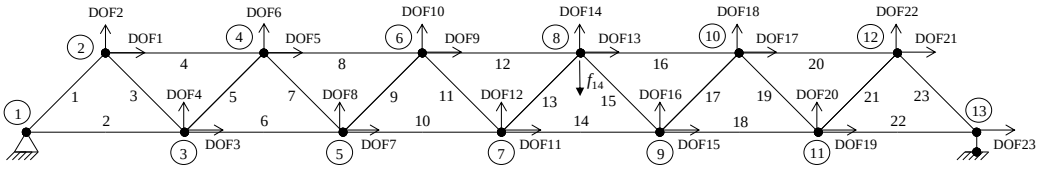

(a) The complete truss model with 23 members

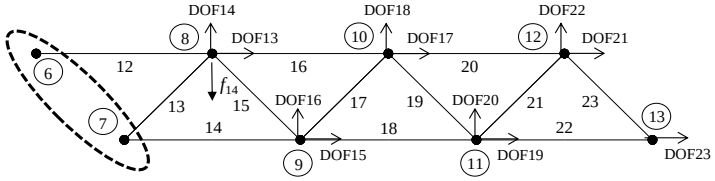

(b) The concerned substructure

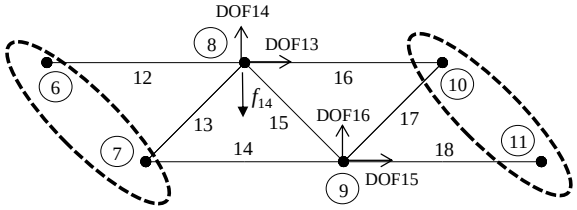

(c) The sub1

Fig. 8 The planar truss model for the numerical example

Table 4 gives the identification results of the corresponding parameters of the sub1 under the various noise levels. It is obvious that as the noise level increases, the identified errors increase as well. However, even the signal is contaminated by 5% noise, the maximum errors for stiffness and damping are respectively 3.27% and 4.56%. The convergence performance for the identification of the parameters of sub1 when the signal is contaminated by 5% noise is shown in Fig. 9 as an example. It can be seen from Fig. 9 that the parameters can be identified through very limited iteration. Moreover, the unknown dynamic loadings applied on the 8th node in this case can be simultaneously identified as well. For the sake of ease and clarity comparison, the time segment of the identified loading from 1s to 1.2s and the relative error during the whole time series are plotted in Fig. 10. It can be easily found that the identified force satisfactorily match with the actual one.

Based on the identified parameters of the sub1 and the dynamic loading mentioned before, the remaining coefficients of the concerned substructure can be then obtained. The state vector for the SSI in this numerical example can be given as,

$$Z = \{x_{13} \quad x_{14} \quad ... \quad x_{23} \quad \dot{x}_{13} \quad \dot{x}_{14} \quad ... \quad \dot{x}_{23} \quad k_{19} \quad k_{20} \quad ... \quad k_{23} \quad c_{19} \quad c_{20} \quad ... \quad c_{23}\}^T_{32\times1} \tag{33}$$

where x_i and $\dot{x}_i$ respectively denotes the displacement and velocity of the i-th DOF; k_i and c_i respectively are the stiffness and damping coefficients of the i-th member to be identified in the concerned substructure.

Table 4 The identified results of the sub1 in the truss model

Parameters	Noise-free		3% noise		5% noise	
	Identified	Error (%)	Identified	Error (%)	Identified	Error (%)
k_{12}	9.60×10^4	0.00	9.47×10^4	1.33	9.37×10^4	2.42
k_{13}	9.00×10^4	0.00	9.02×10^4	0.25	9.04×10^4	0.44
k_{14}	9.20×10^4	0.00	9.17×10^4	0.37	9.14×10^4	0.62
k_{15}	8.40×10^4	0.00	8.41×10^4	0.13	8.42×10^4	0.22
k_{16}	7.60×10^4	0.00	7.46×10^4	1.85	7.35×10^4	3.27
k_{17}	7.60×10^4	0.00	7.55×10^4	0.70	7.51×10^4	1.13
k_{18}	8.60×10^4	0.00	8.64×10^4	0.47	8.65×10^4	0.61
c_{12}	1700.00	0.00	1653.38	2.74	1622.55	4.56
c_{13}	1500.00	0.00	1492.38	0.51	1486.65	0.90
c_{14}	1400.00	0.00	1415.51	1.11	1452.17	3.73
c_{15}	1600.00	0.00	1601.27	0.08	1602.25	0.14
c_{16}	1450.00	0.00	1436.77	0.91	1419.08	2.13
c_{17}	1550.00	0.00	1545.51	0.29	1540.74	0.60
c_{18}	1350.00	0.00	1319.66	2.25	1299.71	3.72

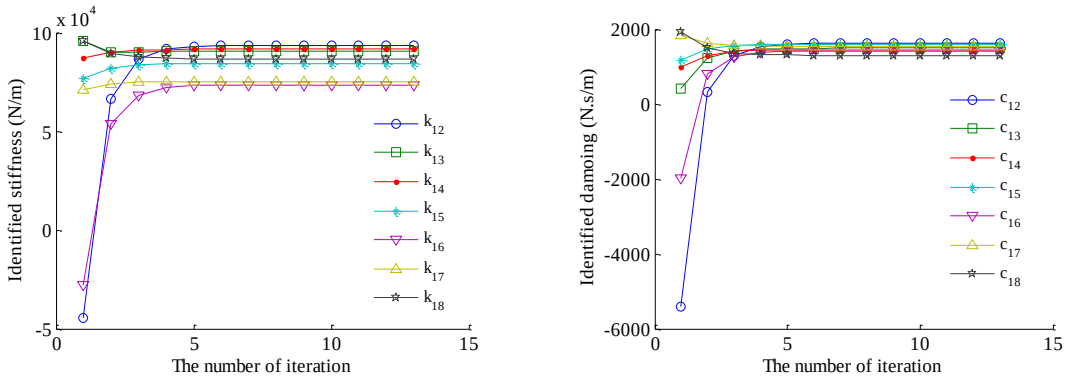

(a) The iteration for identifying stiffness of sub1 (b) The iteration for identifying damping of sub1

Fig. 9 The convergence performance for the parameter identification of the sub1 (5% noise)

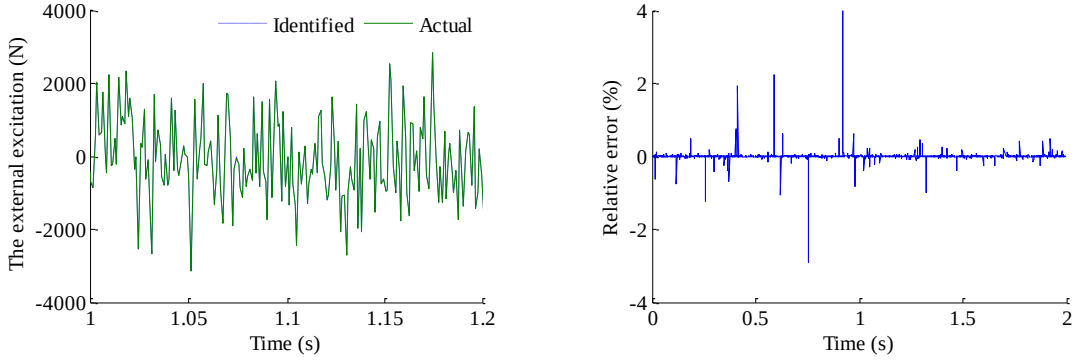

(a) Time segment of the loading (b) The relative identified error

Fig. 10 The comparison of the identified dynamic loading in the truss model (5% noise)

As mentioned before, the responses of the sub1 as well as the boundary are known for the identification. For simplicity, only the displacement and velocity are employed here and the observation equation for the identification of the remaining substructural parameters can be shown as follows

$$y(t) = \{x_9(t) \quad \ldots \quad x_{20}(t) \quad \dot{x}_9(t) \quad \ldots \quad \dot{x}_{20}(t)\}^T \tag{34}$$

Similarly, the initial values of the stiffness and damping are chosen to be 80% of the previously identified one. Moreover, the error covariance matrix is $Q = 0.1 \times I$, and the weight w is set to be 1000 as well. Three noise levels, i.e. noise-free, 3% noise and 5% noise are considered for the identification of the remaining parameters. Based on the state vector shown in Eq. (33) and the observation equation shown in Eq. (34), the remaining parameters of the concerned substructure under those three noise levels are identified and shown in Table 5. The maximum identified errors

for stiffness in the cases of noise-free, 3% noise, and 5% noise are respectively 1.26%, 3.05% and 4.76%. The identified errors for damping are relatively larger with the maximum values of 2.77%, 3.35% and 5.61% in the corresponding three cases.

Moreover, the performance of the first local iteration and the final local iteration on the identification of the stiffness and damping coefficients are respectively shown in Figs. 11 and 12. To avoid redundant comparison, only the identified stiffness and damping coefficients of the 19th truss member when noise level is 5% noise are shown in Figs. 11 and 12. The dashed line represents the actual value whereas the solid line is the corresponding estimated one. For ease and clarity of the comparison, the same scale of the coordinate is employed in both plots. It can be found from Figs. 11 and 12 that in the first local iteration the identified parameters are not correct but seem to be stable. However, as the implementation of the global iteration, the identified parameters are finally close to the actual ones in the last local iteration. Furthermore, the identified results of all these remaining parameters in the global iteration are plotted in Fig. 13 as well. It can be seen that the results in the first several global iterations are not correct, but the identified parameters could be finally converged to the actual one with limited global iterations.

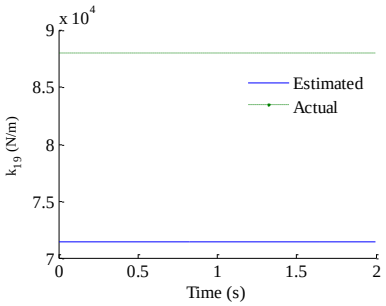

(a) The identified k_{19} in the first local iteration

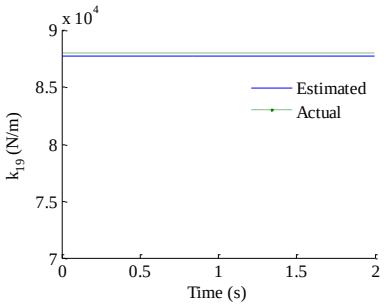

(b) The identified k_{19} in the final local iteration

Fig. 11 The identified $(EA/L)_{19}$ in the local iteration (5% noise)

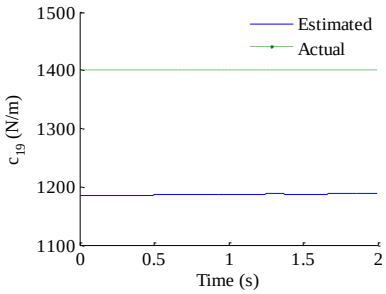

(a) The identified c_{19} in the first local iteration

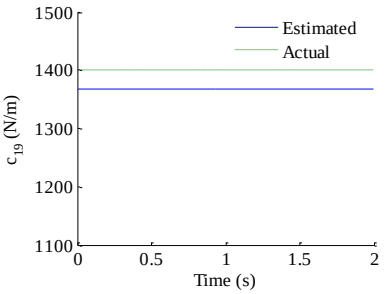

(b) The identified c_{19} in the final local iteration

Fig. 12 The identified c_{19} in the local iteration (5% noise)

Table 5 The identified remaining parameters of the concerned substructure in the truss model

Parameters	Noise-free		3% noise		5% noise	
	Identified	Error (%)	Identified	Error (%)	Identified	Error (%)
$(EA/L)_{19}$	8.82×10^4	0.21	8.94×10^4	1.54	8.78×10^4	0.22
$(EA/L)_{20}$	9.01×10^4	0.05	9.27×10^4	3.05	9.24×10^4	2.69
$(EA/L)_{21}$	7.11×10^4	1.26	7.18×10^4	0.21	7.06×10^4	1.90
$(EA/L)_{22}$	8.45×10^4	0.66	8.56×10^4	1.88	8.01×10^4	4.76
$(EA/L)_{23}$	7.99×10^4	0.09	8.15×10^4	1.83	8.06×10^4	0.70
c_{19}	1396.67	0.26	1377.58	1.60	1367.31	2.33
c_{20}	1515.52	1.03	1534.86	2.32	1566.25	4.42
c_{21}	1210.96	0.91	1222.22	1.85	1227.55	2.30
c_{22}	1264.03	2.77	1343.59	3.35	1360.91	4.68
c_{23}	1254.12	0.33	1254.12	2.64	1320.11	5.61

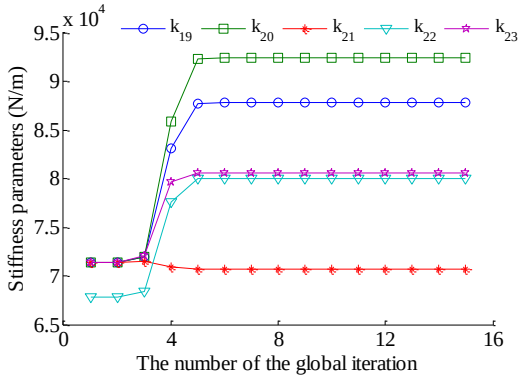

(a) The identified stiffness in the global iteration

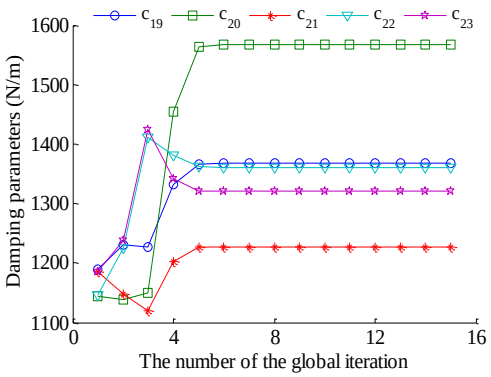

(b) The identified damping in the global iteration

Fig. 13 All the identified remaining parameters in the global iteration (5% noise)

5. Conclusions

In this paper, an alternative substructural identification approach by the combination of weighted adaptive iteration (WAI) approach and an extended Kalman filter method with a weighted global iteration (EFK-WGI) was proposed for simultaneous identification of substructural parameters as well as the unknown external excitations applied on the concerned substructure with limited observations.

In the proposed approach, based on the location of the unknown dynamic loadings and the partially available structural response measurements, a part of structural parameters of the concerned substructure and the unknown loadings were first identified by using the proposed WAI approach. Subsequently, the remaining physical parameters of the concerned substructure were identified by EKF-WGI method using the previously identified loadings and substructural parameters. The feasibility and reliability of the proposed approach was demonstrated via a 20-story shear building structure and a 23 degrees of freedom (DOFs) planar truss model with unknown external excitation and partially known response measurements. Results show that the proposed approach is capable of satisfactorily identifying both the substructural parameters and unknown loading within limited iterations when both the excitation and dynamic response are partially unknown.

Only the structural responses of the DOFs in the sub1 and its interface in terms of acceleration, velocity and displacement are required for the identification of the concerned substructure. Notably, to implement the proposed approach for the identification of the concerned substructure, the selection of the sub1 should be carefully considered to make sure the unknown loadings are applied on it. It can be also seen from the two numerical examples when the complicated boundary involved, for example the boundary of the sub1 in the truss model, the requirement of the measurements for the identification of the concerned substructure are significantly increased. Consequently, for the purpose of the possible real application, the extension and development of the proposed approach for the SSI without the interfacial information could be further carried out. Moreover, it could be found that since the standard least-square estimation algorithm is employed for the identification of the structural parameters, the proposed approach would be impossible to identify the time-variant parameters. However, for practical structural health monitoring, the on-line identification is usually desired. From this point of view, the development of the proposed approach for the identification of time-dependent parameters should be considered in the future.

Acknowledgments

The authors gratefully acknowledge the support provided through the National Natural Science Foundation of China (NSFC) under grant No 50978092.

References

Carden, E.P. and Fanning, P. (2004), "Vibration based condition monitoring: a review", *Struct. Health Monit.*, **3**(4), 355-377.

Chang, P.C., Flatau, A. and Liu, S.C. (2003), "Review paper: health monitoring of civil infrastructure", *Struct. Health Monit.*, **2**(3), 257-267.

Fan, W. and Qiao, P.Z. (2011), "Vibration-based damage identification methods: A review and comparative study", *Struct. Health Monit.*, **10**(1), 83-111.

Koh, C.G., See, L.M. and Balendra, T. (1991), "Estimation of structural parameters in time domain: a substructure approach", *Earthq. Eng. Struct. D.*, **20**(8), 787-801.

Koh, C.G., Hong, B. and Liaw, C.Y. (2003), "Substructural and progressive structural identification methods", *Eng. Struct.*, **25**(12), 1551-1563.

Law, S.S. and Yong, D. (2011), "Substructure methods for structural condition assessment", *J. Sound Vib.*, **330**(15), 3606-3619.

Lei, Y., Wang, H.F. and Shen, W.A. (2012a), "Update the finite element model of Canton Tower based on direct matrix updating with incomplete modal data", *Smart Struct. Syst.*, **10**(4-5), 471-483.
Lei, Y., Jiang, Y.Q. and Xu, Z.Q. (2012b), "Structural damage detection with limited input and output measurement signals", *Mech. Syst. Signal Pr.*, **28**, 229-243.
Li J., Law, S.S. and Ding, Y. (2012), "Substructure damage identification based on response reconstruction in frequency domain and model updating", *Eng. Struct.*, **41**, 270-284.
Li, J. and Law, S.S. (2012), "Substructural Damage Detection With Incomplete Information of the Structure", *J. Appl. Mech.- ASCE*, **79**(4), DOI: 10.1115/1.4005552.
Lu, Z.R., Huang, M. and Liu, J.K. (2011), "State-space formulation for simultaneous identification of both damage and input force from response sensitivity", *Smart Struct. Syst.*, **8**(2), 157-172.
Park, J.H., Kim, J.T., Hong, D.S., Mascarenas, D. and Lynch, P.J. (2010), "Autonomous smart sensor nodes for global and local damage detection of prestressed concrete bridges based on accelerations and impedance measurements", *Smart Struct. Syst.*, **6**(5-6), 711-730.
Park, J.H., Kim, J.T. and Yi, J.H. (2011), "Output-only modal identification approach for time-unsynchronized signals from decentralized wireless sensor network for linear structural systems", *Smart Struct. Syst.*, **7**(1), 59-82.
Rahmatalla, S., Eun, H.C. and Lee, E.T. (2012), "Damage detection from the variation of parameter matrices estimated by incomplete FRF data", *Smart Struct. Syst.*, **9**(1), 55-70.
Tee, K.F., Koh, C.G. and Quek, S.T. (2005), "Substructural first- and second-order model identification for structural damage assessment", *Earthq. Eng. Struct. D.*, **34**(15), 1755-1775.
Tee, K.F., Koh, C.G. and Quek, S.T. (2009), "Numerical and Experimental Studies of a Substructural Identification Strategy", *Struct. Health Monit.*, **8**(5), 397-410.
Trinh, T.N. and Koh, C.G. (2012), "An improved substructural identification strategy for large structural systems", *Struct. Control Health Monit.*, **19**(8), 686-700.
Xu, B. (2005), "Time domain substructural post-earthquake damage diagnosis methodology with neural networks", *Lecture Note in Computer Science*, **3611**, 520-529.
Xu, B., He, J., Rovekamp, R. and Dyke, S.J. (2012), "Structural parameters and dynamic loading identification from incomplete measurements: Approach and validation", *Mech. Syst. Signal Pr.*, **28**, 244-257.
Yi, T.H., Li, H.N. and Gu, M. (2011), "Characterization and extraction of global positioning system multipath signals using improved particle filtering algorithm", *Meas. Sci. Technol.*, **22**(7), Article ID 075101: 1-11.
Yi, T.H., Li, H.N. and Gu, M. (2013a), "Wavelet based multi-step filtering method for bridge health monitoring using GPS and accelerometer", *Smart Struct. Syst.*, 2013, **11**(4), 331-348.
Yi, T.H., Li, H.N. and Sun H.M. (2013b), "Multi-stage structural damage diagnosis method based on energy-damage theory", *Smart Struct. Syst.*, **12**(3-4), 345-361.
Zhang, D.Y. and Johnson, E.A. (2012), "Substructure identification for shear structures: cross-power spectral density method", *Smart Mater. Struct.*, **21**(5), 1-12.
Zhang, D.Y. and Johnson, E.A. (2013), "Substructure identification for shear structures I: Substructure identification method", *Struct. Control Health Monit.*, **20**(5), 804-820.